

Supporting Information

Simulation and measurement of complete dye sensitised solar cells: Including the influence of trapping, electrolyte, oxidised dyes and light intensity on steady state and transient device behaviour

Piers R. F. Barnes*, Assaf Y. Anderson, James R. Durrant and Brian C. O'Regan**

Department of Chemistry, Imperial College London, London SW7 2AZ, U.K.

*piers.barnes@imperial.ac.uk

**b.oregan@imperial.ac.uk

Example of cell showing similar non-ideality for transport and recombination.

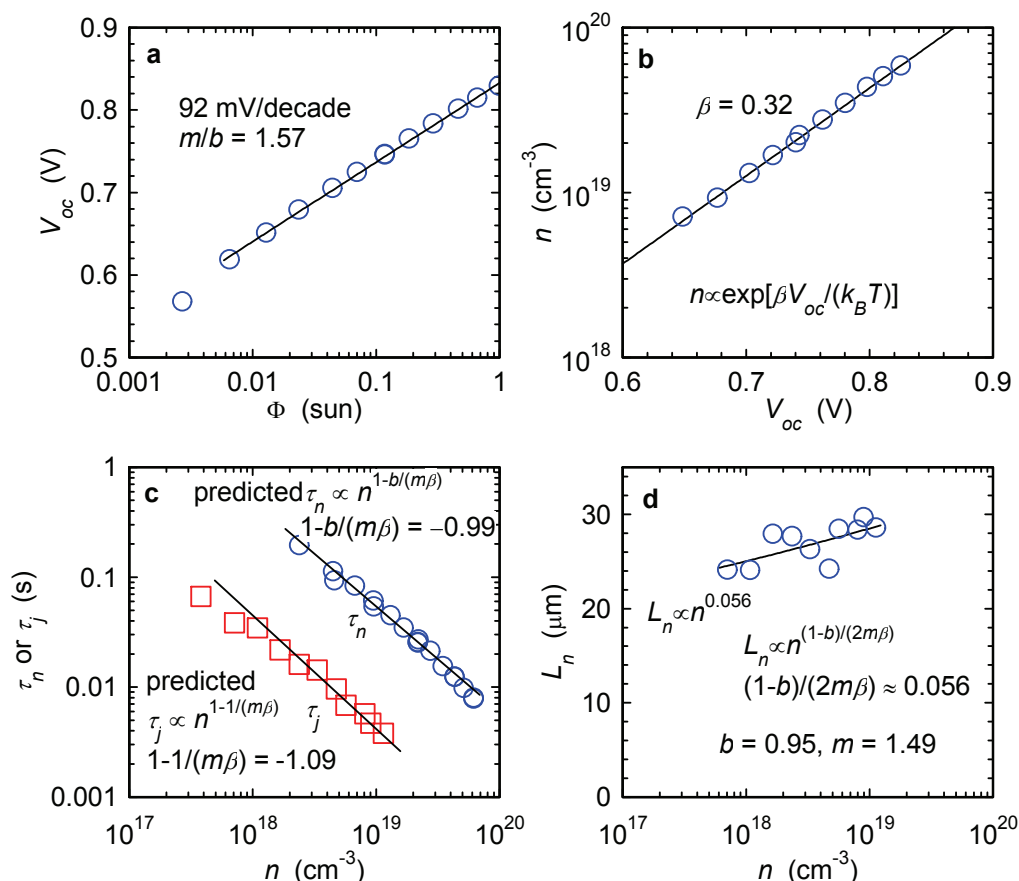


Figure S1. Photoelectrochemical measurements of an N719 sensitised cell, with an MPN electrolyte containing 0.6 M TBAI and 0.1 M iodine, with TiCl_4 treatment, $d = 13 \mu\text{m}$. **a.** Open circuit photovoltage plotted (V_{oc}) against light intensity (Φ), solid line shows a logarithmic fit giving the change in V_{oc} per decade change in Φ , using equation 32 assuming k_{rec} is approximately constant. The value of m/b are given by the ratio of the ideal dependence of V_{oc} on Φ (59 mV) to the observed dependence. **b.** Charge extraction measurements of the concentration of electrons in the cell plotted as a function of V_{oc} , the trap distribution parameter β is derived from the slope of this curve according to equation 12. **c.** Small perturbation photovoltage (τ_n) and photocurrent (τ_j) lifetime measurements measured at different light intensities plotted against charge concentration n . The dashed lines show the slopes predicted by the multiple trapping model by equations 40 and 41. **d.** Transient diffusion lengths calculated using $L_n = (D_n \tau_n)^{1/2}$ from the data in figure c. The solid line show power law fit to the data.

Example of cell showing different non-ideality for transport and recombination.

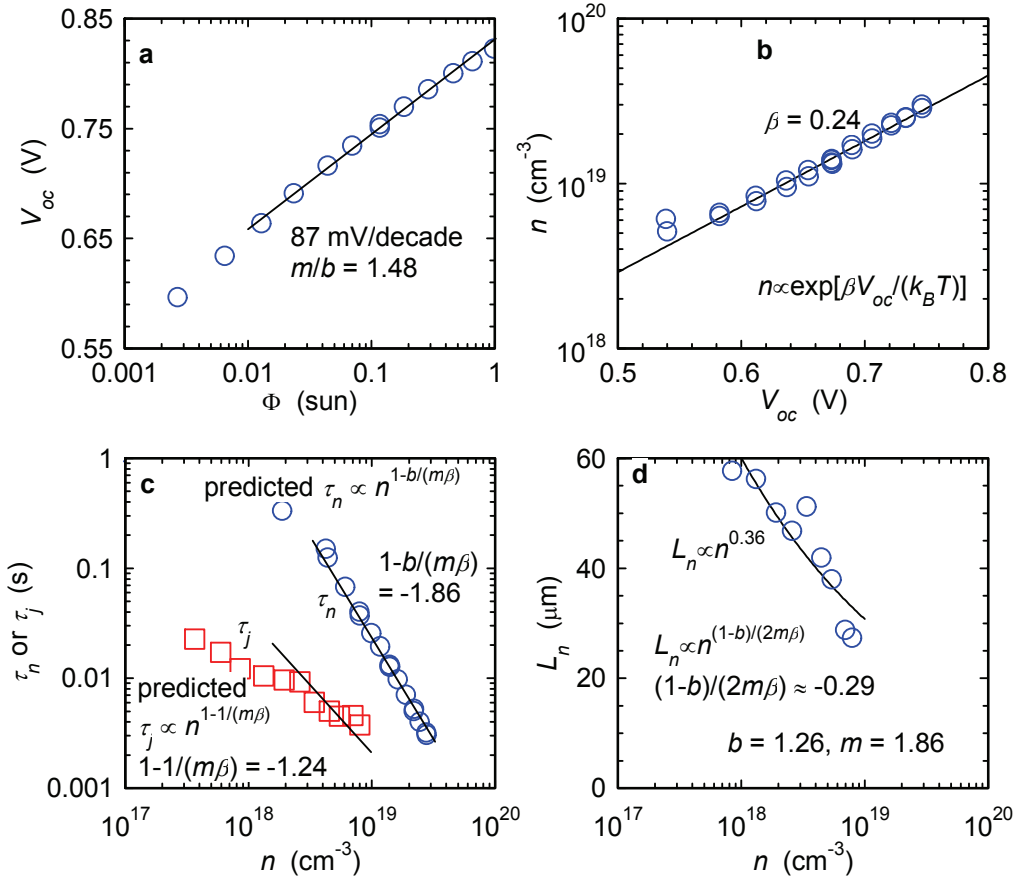


Figure S2. Photoelectrochemical measurements of an N719 sensitised cell, with an MPN electrolyte containing 0.6 M TBAI, 0.1 M iodine, 0.1 M LiI and 0.5 M TBP with no $TiCl_4$ treatment, $d = 13.6 \mu\text{m}$. **a.** Open circuit photovoltage plotted (V_{oc}) against light intensity (Φ), solid line shows a logarithmic fit giving the change in V_{oc} per decade change in Φ , using equation 32 assuming k_{rec} is approximately constant. The value of m/b are given by the ratio of the ideal dependence of V_{oc} on Φ (59 mV) to the observed dependence. **b.** Charge extraction measurements of the concentration of electrons in the cell plotted as a function of V_{oc} , the trap distribution parameter β is derived from the slope of this curve according to equation 12. **c.** Small perturbation photovoltage (τ_n) and photocurrent (τ_j) lifetime measurements measured at different light intensities plotted against charge concentration n . The dashed lines show the slopes predicted by the multiple trapping model by equations 40 and 41. **d.** Transient diffusion lengths calculated using $L_n = (D_n \tau_n)^{1/2}$ from the data in figure c. The solid line show power law fit to the data.

Example of simulated photocurrent transients with differing electron generation profiles from the transient pulse

Figure S3 shows examples of simulated small perturbation photocurrent transients resulting from a strongly absorbed pulse where $ad = 10$ for opposite pulse illumination directions (SE and EE sides) compared with uniformly generated pulses. To simplify the interpretation of the transients the effects of trapping were neglected by setting $N_L = 0$, $b = 1$, $k_{edr} = 0$ and the concentration of electrolyte species were held uniformly constant. The figure clearly indicates that the time constants for the tail of the transients (τ_j) are identical (to within 4 significant figures) in cases where recombination is negligible ($L_n/d = 10$, figure 10a) and where recombination is moderate ($L_n/d = 1$, figure 10b). Furthermore the value of τ_j obtained from these transients correctly predicts the electron diffusion coefficient used for the simulation using the relationship given by equation 35 and the simulation parameter k_{eer} to give τ_n . In cases where recombination coefficient is very significant ($L_n/d = 0.1$, figure 10c) τ_j is weakly dependent on generation profile. This leads to a deviation of the measured diffusion coefficient from the parameterised value, ${}^SD_n/{}^CD_n = 1.35$ for SE side illumination ($ad = 10$), ${}^SD_n/{}^CD_n = 1.05$ for uniform generation and ${}^SD_n/{}^CD_n = 0.86$ for EE side illumination ($ad = 10$). Thus we can conclude that estimation of D_n using transient photocurrent measurements is not significantly influenced by the pulse generation profile in most cases.

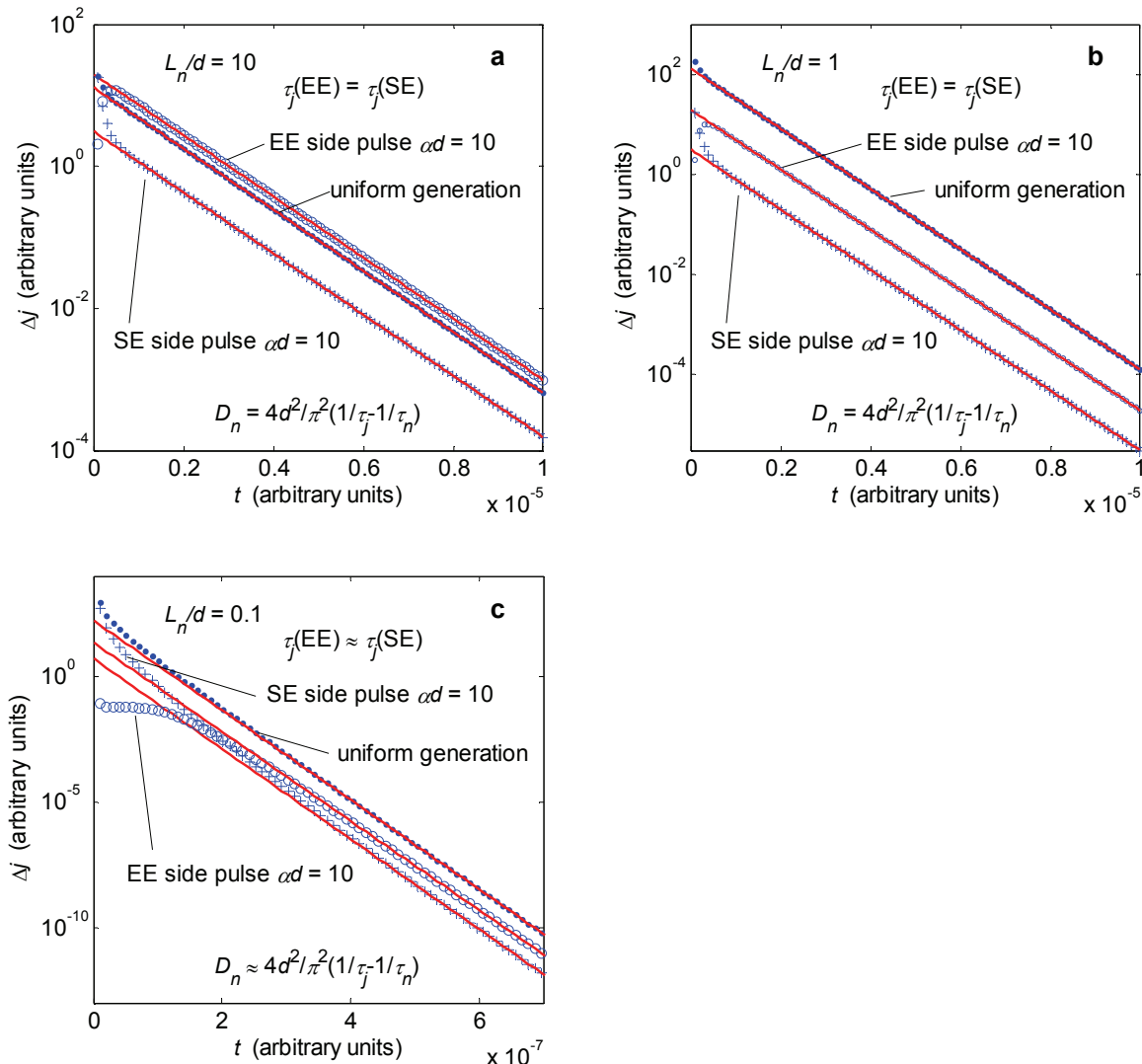


Figure S3. Simulated photocurrent transients when illuminated by a pulse from the SE side (open circles) or EE side (points). In both case the pulse generation profile is highly non-uniform with $\alpha d = 10$. Two case are shown: **a.** where recombination is negligible ($L_n/d = 10$) and **b.** intermediate recombination ($L_n/d = 1$) **c.** where recombination is very significant ($L_n/d = 0.1$). The solid lines show the fits to the tail of the transients using a single exponential. The time constant for the fits, τ_j for both sides in conjunction with the τ_n yields the diffusion coefficient used for the simulation.

Figure S4 shows the consequence of non-uniform generation profiles on the variation in photovoltage rise time constant τ_{rise} .

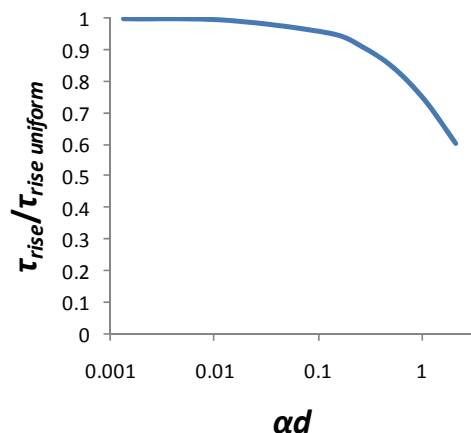


Figure S4. Simulated transient photovoltage rise time constant (τ_{rise}) for as a function of exponential SE side pulse generation profile depth (αd). All rise times are normalised by the rise time for a uniform generation pulse ($\tau_{rise\ uniform}$).